Supplemental Material: Optomechanically Induced Birefringence and Faraday Effect

Robert Duggan,[1] Javier del Pino,[2] Ewold Verhagen,[2] and Andrea Alù[1,3,4,5]

[1]*Department of Electrical and Computer Engineering, The University of Texas at Austin, Austin, TX 78712, USA*

[2]*Center for Nanophotonics, AMOLF, Science Park 104, 1098 XG Amsterdam, The Netherlands*

[3]*Photonics Initiative, Advanced Science Research Center, City University of New York, NY 10031, USA*

[4]*Physics Program, Graduate Center, City University of New York, NY 10016, USA*

[5]*Department of Electrical Engineering, City College of The City University of New York, NY 10031, USA*

SEMICLASSICAL SCATTERING ANALYSIS

Here we detail the derivation of the scattering matrix of the system, starting from the optomechanical Hamiltonian for two degenerate cavity modes $\hat{\mathbf{a}}^T = (\hat{a}_H, \hat{a}_V)$ in the rotating frame of a biasing pump field at frequency ω_L. Setting $\hbar = 1$, this is given by $\hat{H} = \hat{H}_{\rm mec} - \hat{\mathbf{a}}^\dagger \hat{\mathbf{a}}(\Delta + G\hat{x})$, where $\hat{H}_{\rm mec} = \frac{m_{\rm eff}\Omega_m}{2}\hat{x}^2 + \frac{\hat{p}^2}{2m_{\rm eff}}$ for an oscillator with effective mass $m_{\rm eff}$ [1]. Introducing a strong biasing pump via $\hat{H}_{\rm in} \sim \bar{\boldsymbol{\alpha}}^* \cdot \hat{\mathbf{a}} + $H.c. and defining the effective detuning $\tilde{\Delta} = \Delta + 2g_0^2|\bar{\boldsymbol{\alpha}}|^2/\Omega_m$, linearization around the steady state amplitude $\bar{\boldsymbol{\alpha}}$ yields

$$\hat{H}_{\rm eff} = \hat{H}_{\rm mec} - \tilde{\Delta}\delta\hat{\mathbf{a}}^\dagger\delta\hat{\mathbf{a}} - G(\bar{\boldsymbol{\alpha}}\cdot\delta\hat{\mathbf{a}}^\dagger + \boldsymbol{\alpha}^*\cdot\delta\hat{\mathbf{a}})\hat{x}, \quad \text{(S1)}$$

Neglecting mechanical noise, the system evolution under a weak probe $\mathbf{s}_{\rm in}$ follows from the equations of motion:

$$\delta\dot{\hat{\boldsymbol{a}}} = i\left(\tilde{\Delta} - \frac{\kappa}{2}\right)\delta\hat{\mathbf{a}} + iG\bar{\boldsymbol{\alpha}}\hat{x} + \sqrt{\kappa_c}\mathbf{s}_{\rm in}, \quad \text{(S3a)}$$

$$\ddot{\hat{x}} = -\Omega_m^2\hat{x} - \Gamma_m\dot{\hat{x}} + \frac{G}{m_{\rm eff}}\left(\bar{\boldsymbol{\alpha}}^*\cdot\delta\hat{\mathbf{a}} + \text{H.c.}\right). \quad \text{(S3b)}$$

From Eq. (S2), the mechanical oscillations act as sources for the optical modes, with strengths and phases directly related to the steady-state biasing fields. The same holds for the optical forces. Solving in Fourier space for the long-time mechanical amplitudes in Eq. (S3b), Eq. (S3a) reads as $-i\omega\delta\hat{\boldsymbol{a}}(\omega) = i\mathcal{M}(\hat{\boldsymbol{\alpha}})\delta\hat{\boldsymbol{a}}(\omega) + \mathbf{s}_{\rm in}$ with

$$i(\mathcal{M}(\bar{\boldsymbol{\alpha}}) + \mathbf{1}\omega) = \chi_a^{-1}(\omega)\left[\mathbf{1} - G^2\chi_a(\omega)\chi_m(\omega)\left(\bar{\boldsymbol{\alpha}}\bar{\boldsymbol{\alpha}}^\dagger\right)\right], \quad \text{(S3)}$$

where $\chi_m(\omega) = (m_{\rm eff}(\Omega_m^2 - \omega^2) - im_{\rm eff}\Gamma_m\omega)^{-1}$ and $\chi_\alpha(\omega) = (-i(\Delta+\omega) + \kappa/2)^{-1}$ stand for the mechanical and cavity susceptibilities, respectively. Input and output modes are linked by the 2×2 scattering matrix (basis-independent) expression $\mathcal{S}(\omega, \bar{\boldsymbol{\alpha}}) = -\mathbf{1} + i\kappa_c(\mathcal{M}(\bar{\boldsymbol{\alpha}}) + \omega\mathbf{1})^{-1}$. Since $\mathcal{M}(\bar{\boldsymbol{\alpha}})$ can be written as the outer product of two vectors, the inverse follows from the following corollary of the Woodbury matrix identity [2]: for general $\mathbf{u}, \mathbf{v}, (\mathbf{1} + \mathbf{u}\mathbf{v}^T)^{-1} = \mathbf{1} - \mathbf{u}\mathbf{v}^{\mathbf{T}}/(\mathbf{1} + \mathbf{v}^{\mathbf{T}}\mathbf{u})$, hence

$$\mathcal{S} = -\mathbf{1} + \kappa_c\chi_a(\omega)\left[\mathbf{1} - \frac{G^2\chi_a(\omega)\chi_m(\omega)\bar{\boldsymbol{\alpha}}\bar{\boldsymbol{\alpha}}^\dagger}{1 + G^2|\bar{\boldsymbol{\alpha}}|^2\chi_a(\omega)\chi_m(\omega)}\right]. \quad \text{(S4)}$$

An explicit computation of the four matrix elements in the horizontal/vertical polarization (H/V) basis yields

$$\mathcal{S}(\omega, \bar{\boldsymbol{\alpha}})_{HH(VV)} = -1 + \frac{i\kappa_c}{f(|\bar{\boldsymbol{\alpha}}|^2)}\left[m_{\rm eff}\left(\omega^2 - \Omega_m^2 + i\Gamma_m\omega\right)\left(\omega + \tilde{\Delta} + i\frac{\kappa}{2}\right) - G^2|\bar{a}_{V(H)}|^2\right], \quad \text{(S5a)}$$

$$\mathcal{S}(\omega, \bar{\boldsymbol{\alpha}})_{VH(HV)} = \frac{i}{f(|\bar{\boldsymbol{\alpha}}|^2)}\kappa_c G^2\bar{a}^*_{H(V)}\bar{a}_{V(H)}, \quad \text{(S5b)}$$

where $f(|\bar{\boldsymbol{\alpha}}|^2) = \left(\omega + \tilde{\Delta} + i\frac{\kappa}{2}\right)\left[m_{\rm eff}\left(\omega^2 - \Omega_m^2 + i\Gamma_m\omega\right)\left(\omega + \tilde{\Delta} + i\frac{\kappa}{2}\right) - G^2|\bar{\boldsymbol{\alpha}}|^2\right]$.

The expressions above capture arbitrary detuning conditions. In the main text, we consider a red-detuned cavity in the resolved-sideband limit ($\kappa \ll \Omega_m$), where the rotating-wave approximation ($\tilde{\Delta} \simeq -\Omega_m$), simplifies Eq. (S1) to the excitation-conserving interaction $\hat{H}_{\rm eff} \simeq -\tilde{\Delta}\delta\hat{\mathbf{a}}^\dagger\delta\hat{\mathbf{a}} + \Omega_m\hat{b}^\dagger\hat{b} - g_0(\bar{\boldsymbol{\alpha}}\cdot\delta\hat{\mathbf{a}}^\dagger\hat{b} + \text{H.c.})$, using $\hat{x} = x_{\rm ZPF}(\hat{b} + \hat{b}^\dagger)$ and defining $g_0 = G/x_{\rm ZPF}$. In this limit,

$$\delta\dot{\hat{\mathbf{a}}} = -i(\Delta + i\kappa/2)\delta\hat{\mathbf{a}} + ig_0\bar{\boldsymbol{\alpha}}\hat{b} + \mathbf{s}_{\rm in}, \quad \text{(S6)}$$

$$\dot{\hat{b}} = -i(\Omega_m + i\Gamma_m/2)\hat{b} + ig_0\bar{\boldsymbol{\alpha}}^\dagger\cdot\delta\hat{\mathbf{a}}. \quad \text{(S7)}$$

Hence, the $\mathcal{S}$-matrix expressions become equivalent to Eq. (S4) after the replacement $G \to g_0$ and

$$\chi_m(\omega) \to \chi_m^{\rm RWA}(\omega) = \left[-i(\Omega_m + \omega) + \Gamma_m/2\right]^{-1}. \quad \text{(S8)}$$

Note also that Eq. (S5b) clearly shows that the $\mathcal{S}$-matrix becomes nonreciprocal ($\mathcal{S}_{VH} \neq \mathcal{S}_{HV}$) when the steady-state cavity fields have a relative phase difference along two orthogonal axes, such as with the circularly polarized pump used in the main text.

GEOMETRICAL ACTION OF THE SCATTERING MATRIX

In this section we offer a geometrical interpretation of the scattering matrix in Eq. (S4) within the high cooperativity limit ($\mathcal{C} = 4g_0^2|\bar{\boldsymbol{\alpha}}|^2/(\Gamma_m\kappa) \gg 1$) and resonance ($\omega = \Omega_m$). The action of $\mathcal{S}$ on $\mathbf{s}_{\text{in}}$ is thus given by

$$\mathcal{S}(\Omega_m, \bar{\boldsymbol{\alpha}})\mathbf{s}_{\text{in}} \overset{\mathcal{C}\gg 1}{\simeq} -\mathbf{s}_{\text{in}} + \frac{2\kappa_c}{\kappa}\left(\mathbf{s}_{\text{in}} - \langle \mathbf{e}_{\bar{\boldsymbol{\alpha}}}, \mathbf{s}_{\text{in}}\rangle \mathbf{e}_{\bar{\boldsymbol{\alpha}}}\right), \quad \text{(S9)}$$

where $\mathbf{e}_{\bar{\boldsymbol{\alpha}}} = \bar{\boldsymbol{\alpha}}/|\bar{\boldsymbol{\alpha}}|$ is a complex polarization vector for the control field. Neglecting the intrinsic loss channel, $\kappa \simeq \kappa_c$, and Eq. (S9) shows the mapping implemented by $\mathcal{S}$ reflects the input vector over the (complex) control field. In order to determine how this mapping translates into a geometrical operation in the Bloch sphere, the control polarization vector is written as $\mathbf{e}_{\bar{\boldsymbol{\alpha}}} = (\cos\theta_{\mathbf{k}}/2, e^{i\varphi_{\mathbf{k}}}\sin\theta_{\mathbf{k}}/2)$ and the $\mathcal{S}$-matrix is expanded in the Pauli basis as

$$\mathcal{S}(\Omega_m, \bar{\boldsymbol{\alpha}}) = \mathbf{1} - 2\mathbf{e}_{\bar{\boldsymbol{\alpha}}}^{\dagger}\mathbf{e}_{\bar{\boldsymbol{\alpha}}} = -\mathbf{v}_{\bar{\boldsymbol{\alpha}}} \cdot \boldsymbol{\sigma}, \quad \text{(S10)}$$

where $\mathbf{v}_{\bar{\boldsymbol{\alpha}}} = \left(\, \sin\theta_{\mathbf{k}}\cos\varphi_{\bar{\boldsymbol{\alpha}}},\ \sin\theta_{\mathbf{k}}\sin\varphi_{\bar{\boldsymbol{\alpha}}},\ \cos\theta_{\bar{\boldsymbol{\alpha}}}\,\right)$ is the 3-vector representing the control field in the Poincaré sphere and $\boldsymbol{\sigma} = (\sigma_x, \sigma_y, \sigma_z)$. This procedure effectively allows to switch from a (complex) $SU(2)$ representation to a (real) $O(3)$ representation, in which the scattering transfomation of the input state occurs via a similarity transform $\mathcal{S}(\mathbf{v}_{\text{in}} \cdot \boldsymbol{\sigma})\mathcal{S}^{\dagger}$, which can be expressed as

$$\mathbf{v}_{\text{out}} \cdot \boldsymbol{\sigma} = \left[-\mathbf{v}_{\text{in}} + 2\left(\mathbf{v}_{\text{in}} \cdot \mathbf{v}_{\theta,\varphi}\right)\mathbf{v}_{\bar{\boldsymbol{\alpha}}}\right] \cdot \boldsymbol{\sigma}. \quad \text{(S11)}$$

Here we exploited the relation $(\mathbf{a}\cdot\boldsymbol{\sigma})(\mathbf{b}\cdot\boldsymbol{\sigma})(\mathbf{a}\cdot\boldsymbol{\sigma}) = -(\mathbf{a}\cdot\boldsymbol{\sigma}) + 2(\mathbf{a}\cdot\mathbf{b})(\mathbf{b}\cdot\boldsymbol{\sigma})$, for $\mathbf{a}, \mathbf{b} \in \mathbb{R}^3$. Since we are free to choose the representation for $\boldsymbol{\sigma}$, the general expression

$$\mathbf{v}_{\text{out}} = -\mathbf{v}_{\text{in}} + 2\left(\mathbf{v}_{\bar{\boldsymbol{\alpha}}} \cdot \mathbf{v}_{\text{in}}\right)\mathbf{v}_{\bar{\boldsymbol{\alpha}}}, \quad \text{(S12)}$$

must hold. Eq. (S12) is a particular case of the Rodrigues rotation formula for a real 3-vector around an axis $\mathbf{v}_{\bar{\boldsymbol{\alpha}}}$ and angle $\epsilon = \pi$ [3], given by $\mathbf{a}_{\text{rot}} = \mathbf{a}\cos\epsilon + (\mathbf{v}_{\bar{\boldsymbol{\alpha}}} \times \mathbf{a})\sin\epsilon + \mathbf{v}_{\bar{\boldsymbol{\alpha}}}(\mathbf{v}_{\bar{\boldsymbol{\alpha}}} \cdot \mathbf{a})(1 - \cos\epsilon) = -\mathbf{a} + 2(\mathbf{v}_{\bar{\boldsymbol{\alpha}}} \cdot \mathbf{a})\mathbf{v}_{\bar{\boldsymbol{\alpha}}}$. This formula outputs the rotated vector by decomposing the input into its components parallel and perpendicular to $\mathbf{v}_{\bar{\boldsymbol{\alpha}}}$ and rotating only the perpendicular component.

SCATTERING AT FINITE PUMP DETUNING

As discussed in the main text, a primary effect of detuning of the control field from the mechanical sideband is a weakened optomechanical interaction. This results in varying output amplitude and phase for the reflection component of the signal parallel to the control field. In the following discussion we consider a real control and probe polarization axes for the sake of simplicity. In particular, in the limit of vanishing optical absorption ($\kappa \simeq \kappa_c$) and negligibly damped mechanical resonator ($\Gamma_m \ll \kappa_c$), we recover under an H-polarized control, an approximate phase $\varphi(\tilde{\delta}) = \arg\left[\mathcal{S}_{HH}(\Omega_m - \delta, \bar{\boldsymbol{\alpha}} \parallel \mathbf{e}_H)\right]$ that only depends on the dimensionless quantity $\tilde{\delta} = \delta/\Gamma_m$, which parametrizes the control field detuning, and the cooperativity $\mathcal{C}$. For a probe frequency centered on the optical resonance and neglecting terms $\mathcal{O}(\Gamma_m/\kappa_c)$,

$$\varphi(\tilde{\delta}) \simeq \tan^{-1}\left[\frac{-4\mathcal{C}\tilde{\delta}}{(\tilde{\delta} + \frac{1}{2}\sqrt{\mathcal{C}^2 - 1})(\tilde{\delta} - \frac{1}{2}\sqrt{\mathcal{C}^2 - 1})}\right]. \quad \text{(S13)}$$

The reflection phase thus approaches π as the resonance is crossed ($\tilde{\delta} \to 0$) in the limit $\mathcal{C} \gg 1$, recovering results from the previous section, while $\varphi(\tilde{\delta}_0) \simeq \pm\pi/2$ when $\tilde{\delta}_0 = \pm\sqrt{\mathcal{C}^2 - 1}/2$. This gives a good sense of the cooperativity-dependent resonance width. Such variable phase difference $\varphi(\tilde{\delta}) \in (0, 2\pi)$ is responsible for the behavior shown in Fig. 2 in the main text, where for instance a 45° control field converts $H \to V$ on resonance, while being able to access elliptical states off resonance.

CIRCULATOR DISCUSSION

Utilizing polarization-dependent interactions, we can create a circulator with a CP pump and a two-sided cavity, as shown in the main text. The starting point consists of an unpumped, lossless cavity that transmits all fields on resonance and is thus reciprocal. An RHCP pump then induces reflection of for RHCP probe signals, with strength and bandwidth proportional to the cooperativity. We offer here a quick reminder that we define RHCP as a field component $(\mathbf{e}_H + i\mathbf{e}_V)/\sqrt{2}$ without regard for propagation direction. With the setup of Fig. 3d, in the high cooperativity regime, the H input from both sides of the resonator is converted to RHCP by the QWP, reflected from the resonator, and converted to V by a second pass through the QWP on the same side. The V input instead can pass through the resonator as LHCP light, and passes through the opposite H port. Thus, on resonance, there is circulation between ports $1 \to 2 \to 3 \to 4 \to 1$, shown clearly in Fig. S1.

[1] W. Bowen and G. J. Milburn, *Quantum optomechanics* (CRC press, 2015).

[2] M. S. Bartlett, "An inverse matrix adjustment arising in discriminant analysis," Ann. Math. Statist. **22**, 107–111 (1951).

[3] R. W. Brockett, in *Mathematical Theory of Networks and Systems*.

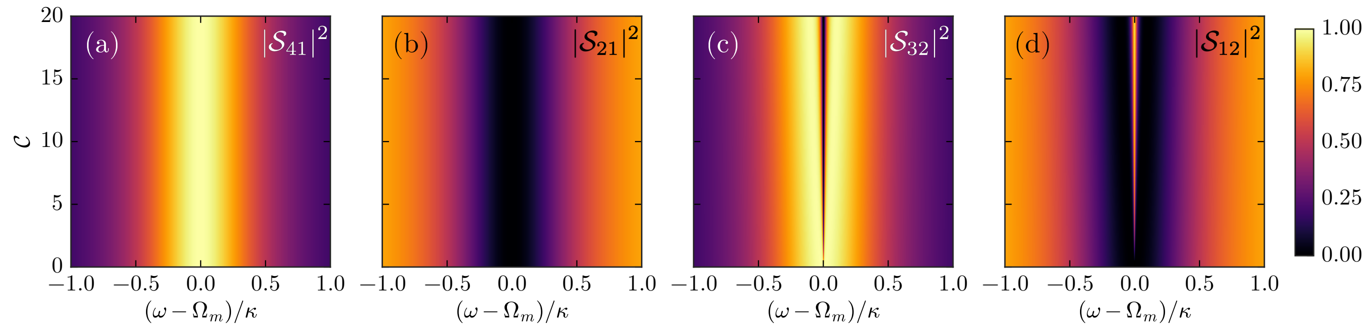

FIG. S1. $\mathcal{S}$-matrix amplitudes for the circulator geometry sketched in the main text with an RH control field. The H input probe fields become RH after passing through the QWP, and exhibit reflection on the mechanical sideband as the cooperativity increases, leaving through the V port on the same side. The V fields however pass through the cavity on resonance, independent of pump power. The coefficients $|\mathcal{S}_{23}|$, $|\mathcal{S}_{43}|$, $|\mathcal{S}_{14}|$, and $|\mathcal{S}_{34}|$ are equal to $|\mathcal{S}_{41}|$, $|\mathcal{S}_{21}|$, $|\mathcal{S}_{32}|$, and $|\mathcal{S}_{12}|$, respectively. For these plots, $\Gamma_m = \Omega_m/5000$ and $\kappa = \kappa_c = \Omega_m/10$.